Composition-dependent structural transition in epitaxial $Bi_{1-x}Sb_x$ thin films on Si(111)

Emily S. Walker,[1] Sarah Muschinske,[1] Christopher J. Brennan,[1] Seung Ryul Na,[2] Tanuj Trivedi,[1] Stephen D. March,[1] Yukun Sun,[3] Tianhao Yang,[2] Alice Yau,[1] Daehwan Jung,[4] Andrew F. Briggs,[1] Erica M. Krivoy,[1] Minjoo L. Lee,[3] Kenneth M. Liechti,[2] Edward T. Yu,[1] Deji Akinwande,[1] and Seth R. Bank[1,*]

[1]*Microelectronics Research Center and Department of Electrical and Computer Engineering, The University of Texas at Austin, Austin, Texas 78758, USA*

[2]*Research Center for the Mechanics of Solids, Structures and Materials and Department of Aerospace Engineering and Engineering Mechanics, The University of Texas at Austin, Austin, Texas 78712, USA*

[3]*Electrical and Computer Engineering Department, The University of Illinois at Urbana-Champaign, Urbana, Illinois 61801, USA*

[4]*Institute for Energy Efficiency, University of California at Santa Barbara, Santa Barbara, California 93106, USA*

(Received 15 May 2018; revised manuscript received 18 July 2018; published 7 June 2019)

Bismuth-antimony alloys ($Bi_{1-x}Sb_x$) are topological insulators between 7 and 22% Sb in bulk crystals, with an unusually high conductivity suitable for spin-orbit torque applications. Reducing the thickness of epitaxial $Bi_{1-x}Sb_x$ films is expected to increase the maximum band gap through quantum confinement, which may improve isolation of topological surface-state transport. Like Bi(001) on Si(111), $Bi_{1-x}Sb_x$ has been predicted to form a black phosphoruslike allotrope with unique electronic properties in nanoscale films; however, the impact of Sb alloying on both the bulklike and nanoscale crystal structures on Si(111) is currently unknown. Here we demonstrate that the allotropic transition in ultrathin epitaxial $Bi_{1-x}Sb_x$ films on Si(111) is suppressed above 8–9% Sb, resulting in an unexpected (012) orientation within the topologically insulating regime. The metallic temperature-dependent conductivity associated with surface states in Bi(001) was not observed in the $Bi_{1-x}Sb_x$(012) films, suggesting that the (012) orientation may significantly reduce surface-state transport. Growth on a Bi(001) buffer layer may prevent this orientation transition. Finally, we demonstrate that Sb alloying improves the continuity and quality of nanoscale $Bi_{1-x}Sb_x$(012) films in the thickness regime expected for the black phosphorus allotrope, suggesting a promising route to large-area growth of puckered-layer two-dimensional $Bi_{1-x}Sb_x$, which will be necessary to harness its unique electronic properties in practical applications.

DOI: 10.1103/PhysRevMaterials.3.064201

I. INTRODUCTION

While topologically insulating $Bi_{1-x}Sb_x$ [1,2] has been less extensively studied than the bismuth chalcogenide [3–9] and ternary [10] three-dimensional topological insulators (TIs) due to its relatively complex surface-state dispersion and small bulk band gap [11–15], it has recently become the focus of renewed research interest due to both its suitability among TIs for spin-orbit torque switching applications [16,17], as well as the prediction of unique physical phenomena at the *L*-band inversion point [18,19]. Quantum confinement, which induces semiconductorlike transport in bismuth (Bi) films below approximately 100 nm [20–22], is predicted to become significant in $Bi_{1-x}Sb_x$ at comparable thicknesses [23]. This has been reported to increase the maximum band gap and extend the semiconducting composition regime [16], which, combined with increased surface to volume ratio in thin films [24], may improve isolation of surface-state contributions to transport, enabling new applications utilizing topological surface states.

Single-monolayer (ML) $Bi_{1-x}Sb_x$ has been predicted to form a (012)-oriented (using the trigonal Bi unit cell) puckered-layer allotrope [25] with an A17 crystal structure similar to black phosphorus [26], suggesting that a thickness-dependent allotropic transition analogous to epitaxial Bi on Si(111) [27–30] may occur in ultrathin films. Two-dimensional (2D) puckered-layer Bi(012) exhibits distinct electronic properties from both the (001)- and (012) orientations of the bulk A7 structure, including decreased metallicity [31], an ~0.3-eV band gap in single monolayers [32] and nanoribbons [33], and increased spin splitting [31]. If puckered-layer $Bi_{1-x}Sb_x$ is stable, it is likely to similarly exhibit unique electronic properties, and to facilitate compositional tuning of the A17 Bi band structure. While bulklike epitaxial $Bi_{1-x}Sb_x$ on Si(111) has been demonstrated [15,24], it is unclear how Sb alloying affects the allotropic transition. Understanding the growth of $Bi_{1-x}Sb_x$/Si(111) is therefore important not only for the integration of TI $Bi_{1-x}Sb_x$ with conventional integrated circuit technology, but also for exploring the properties of 2D puckered-layer $Bi_{1-x}Sb_x$.

In this paper, we report the epitaxial growth of $Bi_{1-x}Sb_x$ films within the expected A7 and A17 thickness regimes on Si(111). We demonstrate using high-resolution x-ray diffraction (XRD) that $Bi_{1-x}Sb_x$(001) films above the critical thickness for A7 Bi(001) (~4 nm) become (012) oriented at compositions of more than 8–9% Sb, coinciding with the onset of the expected TI regime. This (012) orientation is consistent

*sbank@ece.utexas.edu

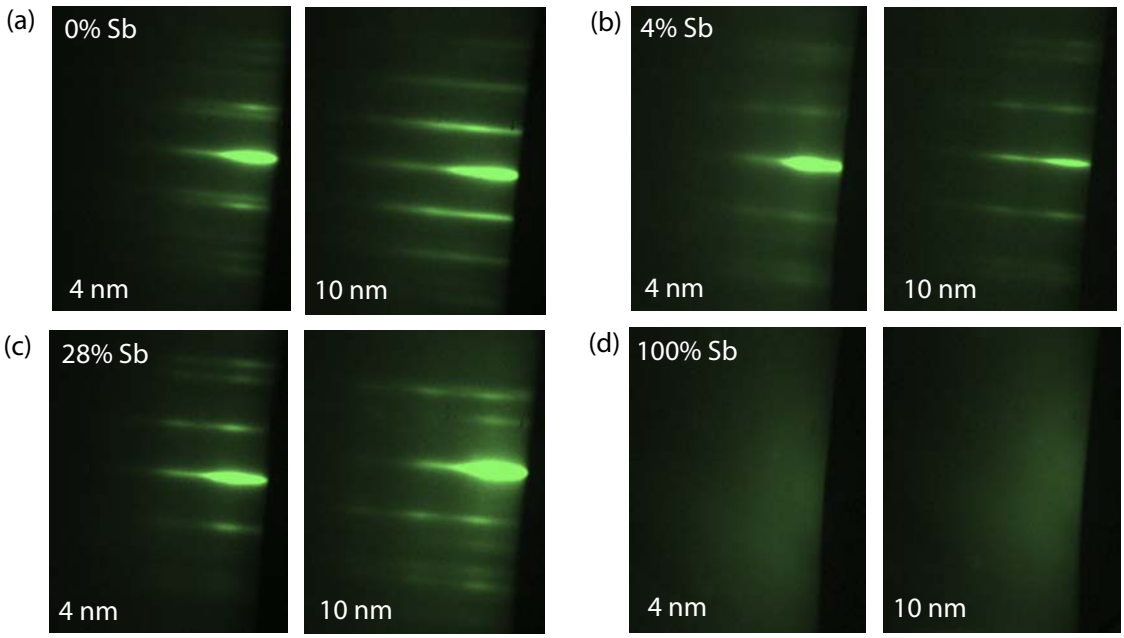

FIG. 1. *In situ* RHEED measurements of (a) Bi, (b) $Bi_{0.96}Sb_{0.04}$, (c) $Bi_{0.72}Sb_{0.28}$, and (d) Sb films indicating change in RHEED between 4 and 10 nm with increasing % Sb.

with thickness, indicating that there is no early nucleation of the A7 (001) phase; rather, the puckered-layer A17 structure likely evolves into the (012)-oriented A7 structure in thicker films. While $Bi_{1-x}Sb_x$(001) films demonstrate the metallic temperature-dependent conductivity characteristic of conductive surface states as the film thickness is reduced [16,24,34], this effect is not observed in $Bi_{1-x}Sb_x$(012), indicating that identification of the surface states through transport measurements may be limited in TI $Bi_{1-x}Sb_x$/Si(111). XRD measurements of Bi/$Bi_{1-x}Sb_x$ superlattices suggest that growth on a Bi buffer layer [15] assists in maintaining the (001) orientation within the TI regime, although such an approach may also complicate electrical measurements.

The consistent weak adhesion of $Bi_{1-x}Sb_x$(001) films to Si(111) [35], as well as the (012) orientation of $Bi_{1-x}Sb_x$ films thinner than ∼4 nm, suggests that the early growth of $Bi_{1-x}Sb_x$/Si(111) is quite similar to Bi, and that the 2D A17 structure is likely achievable. Surprisingly, atomic force microscopy (AFM) and conductivity measurements of nanoscale $Bi_{1-x}Sb_x$(012) indicate that the quality of ultrathin films is significantly improved compared to Bi(012) by an autosurfactant effect [36,37] related to reduced adatom mobility [38]. By facilitating earlier coalescence of few-ML islands, Sb alloying enables electrical measurements of $Bi_{1-x}Sb_x$(012) films thinner than can be measured in Bi(012).

II. RESULTS

$Bi_{1-x}Sb_x$ films between 0 and 100% Sb and 2–50 nm were grown on intrinsic Si(111) substrates using molecular-beam epitaxy in a Varian Gen II system at a substrate temperature of 15–25 °C, with 5-rpm substrate rotation in plane during growth. A downward-looking Veeco Sumo cell was used to deposit 6N Bi source material (<1-ppm impurities), while a Veeco valved cracker source was used to deposit 6N5 Sb (<5-ppm impurities). A total beam equivalent pressure of 2×10^{-7} Torr, including both Bi and Sb, was used for all $Bi_{1-x}Sb_x$ films, corresponding to a growth rate of 0.5 Å/s. As the crystal structure varies with the film thickness, growth rates were calibrated using Å/s units, rather than converting to flux. The Si native oxide was removed prior to growth using hydrofluoric acid, followed by baking *in situ* at 760 °C to desorb the hydrogen passivation. The $Bi_{1-x}Sb_x$ composition was calibrated *ex situ* using x-ray photoelectron spectroscopy (XPS) and electron dispersion spectroscopy acquired with transmission electron microscopy [39]. All $Bi_{1-x}Sb_x$ measurements were conducted on material taken from the center area of the wafer in order to avoid compositional variation across the diameter of the 3-in. wafers, which we found to be significant. Pure Bi films were grown at rates between 0.03 and 0.5 Å/s, which was found necessary to avoid surface droplet formation.

Reflective high-energy electron diffraction (RHEED) measurements acquired *in situ* for 10-nm $Bi_{1-x}Sb_x$ films are shown in Fig. 1. Between 4 and 8 nm (12–24 ML) of pure Bi growth, the RHEED transitioned from a double-lined pattern to a 1 × 1 reconstruction [Fig. 1(a)]. As this RHEED change is associated with the A17 to A7 allotropic transformation [27], the similarity of the 4–28% $Bi_{1-x}Sb_x$ films [Figs. 1(b) and 1(c)] at 4 nm suggests a consistent nanoscale structure in $Bi_{1-x}Sb_x$. However, unlike the pure Bi film, the transition to the 1 × 1 reconstruction is suppressed by Sb alloying; only a partial 1 × 1 reconstruction formed in the 10-nm 4% film [Fig. 1(b)], and no transition was apparent in the 10-nm 28% film. This is consistent with the observation by Hirahara *et al.* of the disappearance of the 1 × 1 reconstruction in $Bi_{1-x}Sb_x$/Si(111) between 22 and 32% Sb [24]. The very hazy RHEED of the Sb film in Fig. 1(d), typical of an amorphous film, suggests that the film quality degraded with increasing Sb, likely due to lower adatom mobility [38]; in fact, we

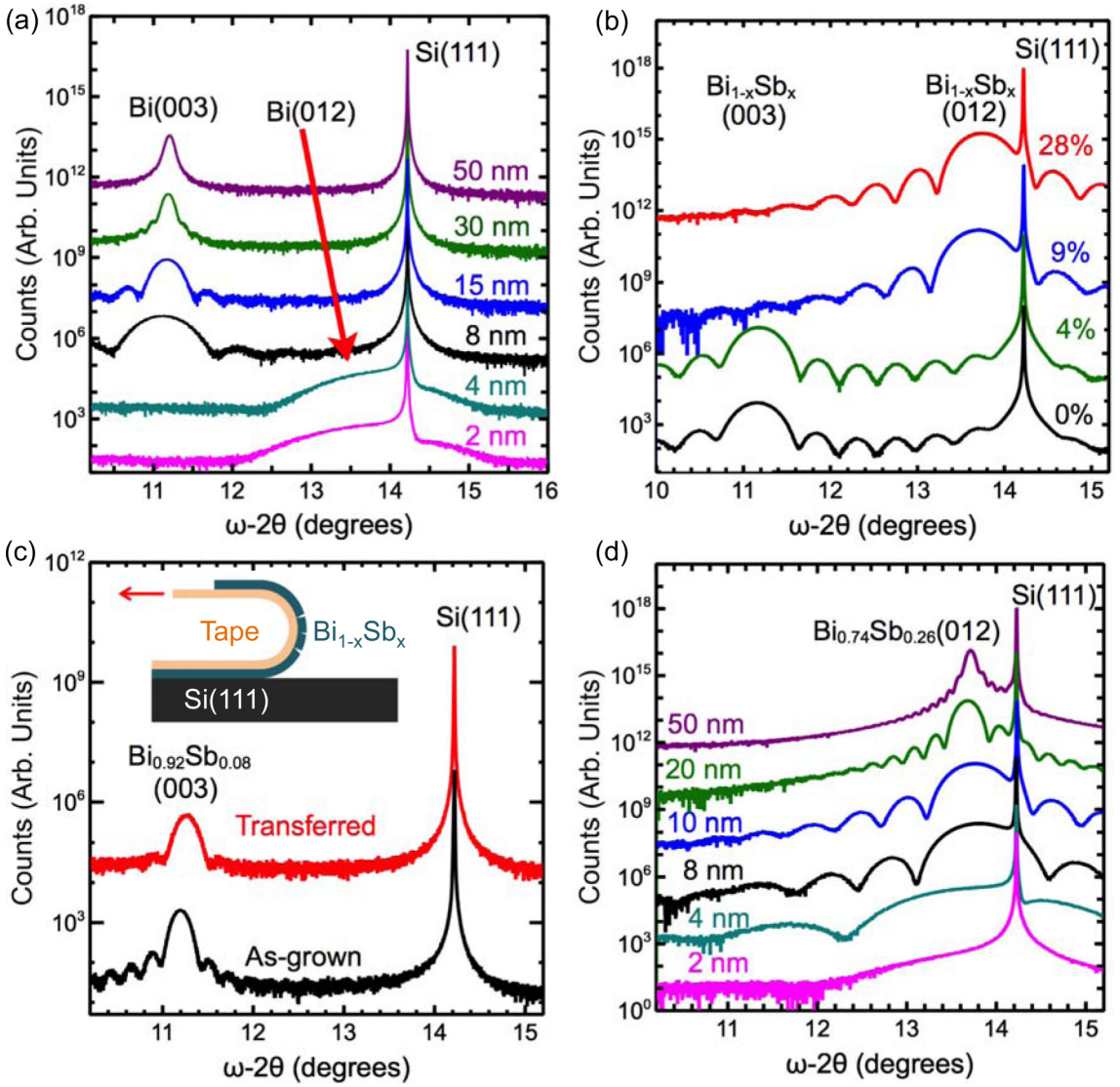

FIG. 2. XRD measurements of (a) thickness-dependent structure of Bi, (b) composition-dependent transition in 10-nm $Bi_{1-x}Sb_x$, (c) $Bi_{1-x}Sb_x(001)$ transferred using thermal release tape (inset), and (d) thickness-dependent $Bi_{0.74}Sb_{0.26}$.

found that a higher substrate temperature was required for high-quality Sb growth, consistent with Sb on germanium [40].

While the structure of $Bi_{1-x}Sb_x(111)$ in the bulklike thickness regime has been previously assumed to be consistent with A7 Bi(001) up to 32% Sb [24], we demonstrate through XRD measurements in Fig. 2 that the film orientation transitions at ∼8–9% Sb. As these XRD measurements are conducted *ex situ*, control Bi samples capped with poly(methyl methacrylate) (PMMA) were used to confirm that the observed orientation transition is not caused by oxidation. Figure 2(a) illustrates the expected thickness-dependent structural transition in Bi reference films from Bi(012) below 4 nm to Bi(001) above 8 nm, in agreement with the observed RHEED transition. This orientation transition indicates that the established thickness-dependent allotropic transition from the A17 (012) to the A7 (001) structure is very likely occurring in pure Bi [27,28,30]. In Fig. 2(b), we find that Sb alloying in 10-nm $Bi_{1-x}Sb_x$ films, well above the critical thickness for the A7(001) structure in Bi, actually induces a second, composition-dependent orientation change from $Bi_{1-x}Sb_x(001)$ to $Bi_{1-x}Sb_x(012)$ between 4 and 9% Sb. Considering the (001) orientation of the somewhat thicker $Bi_{0.92}Sb_{0.08}$ sample shown in Fig. 2(c), which is found to be consistent between 8 and 30 nm, we conclude that the transition occurs between 8 and 9% Sb. The similar (003) peak position in the 4–9% $Bi_{1-x}Sb_x$ films compared to pure Bi is consistent with Vegard's law, which has been previously shown to accurately describe the lattice constant of epitaxial $Bi_{1-x}Sb_x$ [41]. As an orientation change with increasing % Sb has not been reported in $Bi_{1-x}Sb_x$ thin films on other substrates, including gallium arsenide [16] and cadmium telluride [41], this phase transition may be specific to growth on Si(111). Like Bi(001), low-Sb $Bi_{1-x}Sb_x(001)$ films are found in Fig. 2(c) to exhibit unusually weak adhesion to the Si(111) substrate [35], allowing high-quality transfer of structurally intact films using a simple thermal release tape method (shown in inset) adapted from chemical vapor deposition-grown graphene [42]. This weak adhesion suggests that the growth of $Bi_{1-x}Sb_x(001)$ is very similar to Bi(001) on Si(111), and can enable types of applications

based on the integration of $Bi_{1-x}Sb_x(001)$ with arbitrary substrates.

Further insight into the origin of the orientation transition in $Bi_{1-x}Sb_x$ with >9% Sb is provided by thickness-dependent XRD measurements of $Bi_{0.74}Sb_{0.26}$ in Fig. 2(d). In contrast to the pure Bi films, the (012) orientation of $Bi_{0.74}Sb_{0.26}$ is independent of the film thickness, suggesting that nucleation of the (001)-oriented A7 structure, which has been predicted to drive the allotropic transition [29], does not occur. This A7(001) suppression could be related either to breakdown of the Bi(001)/Si(111) coincidence alignment [27,28,43] as the lattice constant is reduced by Sb alloying [43], or to lowered adatom mobility [38], which will be discussed later. The A17 crystal structure is very similar to the pseudocubic (012)-oriented A7 structure of Bi, with differences arising from layer pairing in nanoscale films to reduce the surface energy from dangling bonds [27,29]. As the film thickness increases and surface energy minimization becomes less critical, it is likely that the A17 structure gradually transitions to the A7(012) structure; however, as the d spacing between the two structures is very similar, the critical thickness cannot be distinguished by XRD.

The (012) orientation is likely to significantly impact transport in the $Bi_{1-x}Sb_x$ films due to changes both in the amount of quantum confinement, which is determined by the effective mass in the growth direction [44,45], and in the surface states [46,47]. While the A7 Bi(012) surface also demonstrates spin-split surface states [46,48], the surface-state dispersion is quite different from Bi(001) [46,47], and is more metallic due to the higher density of broken bonds on the (012) surface [27,48,49]. The effect of Sb alloying on Bi(012) surface states is also currently unknown. In order to determine how the orientation impacts electronic properties in A7 $Bi_{1-x}Sb_x$, temperature-dependent sheet conductance [$G_{sh}(T)$] and conductivity measurements of >8-nm films are compared in Fig. 3. In Fig. 3(a), $G_{sh}(T)$ for reference Bi(001) films was found to be consistent with previous reports, and characteristic of coexisting quantum confined bulk and conductive surface states [16,22,34]. Although bulk Bi is semimetallic, G_{sh} for >15-nm films increases with increasing temperature, typical of a semiconducting film, due to quantum confinement of the bulk states. The change in the temperature dependence as the film thickness is reduced below 15 nm is attributed to increasing contributions from metallic surface states in thinner films [16,34]. $Bi_{1-x}Sb_x(001)$ films in Fig. 3(b), which contain less than 9% Sb, demonstrate a similar transition in $G_{sh}(T)$ as the film thickness is reduced; the larger change in G_{sh} in the 20-nm film is consistent with the expected increase in the indirect band gap between T and L due to Sb alloying [1,23]. The similar metallic temperature dependence of the 10-nm film is consistent with measurements of $Bi_{1-x}Sb_x(001)$ on other substrates [16], and suggests that surface states remain present.

In contrast, as the normalized conductivity of 10-nm $Bi_{1-x}Sb_x$ films in Fig. 3(c) illustrates, the 10-nm $Bi_{1-x}Sb_x(012)$ films do not exhibit the metallic temperature dependence expected for surface states; instead, a semiconducting temperature dependence corresponding to the onset of the (012) orientation is observed, which is consistent with film thickness. This result is surprising, given the metallic nature of the Bi(012) surface observed in *in situ* angle resolved photoemission spectroscopy (ARPES) [49]. One possibility is that, due to either the higher density of dangling bonds on the (012) surface or the larger concentration of Sb, the $Bi_{1-x}Sb_x(012)$ surface states are less robust to oxidation

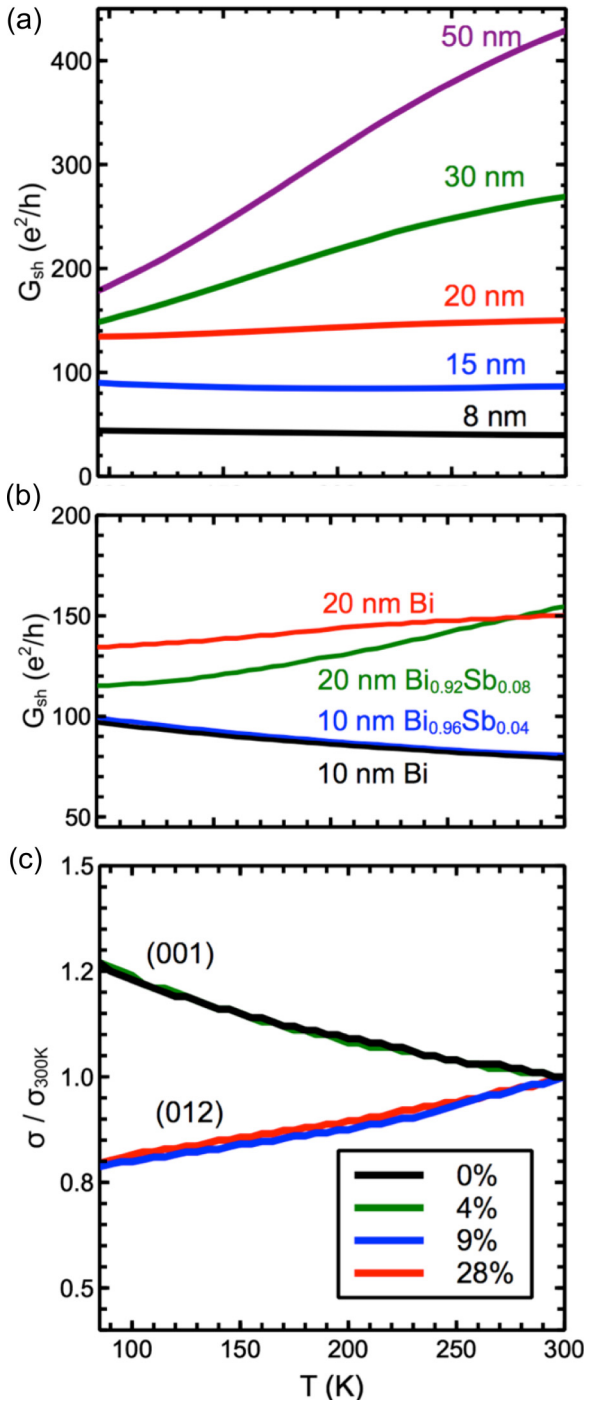

FIG. 3. (a) Sheet conductance measurements of reference Bi(001) films showing shift to metallic temperature dependence below 15 nm. (b) Sheet conductance comparison between Bi(001) and $Bi_{1-x}Sb_x(001)$ indicating consistent thickness-dependent behavior. (c) Conductivity measurements of 10-nm $Bi_{1-x}Sb_x(001)$ films normalized to 300 K indicating change in temperature dependence with orientation transition.

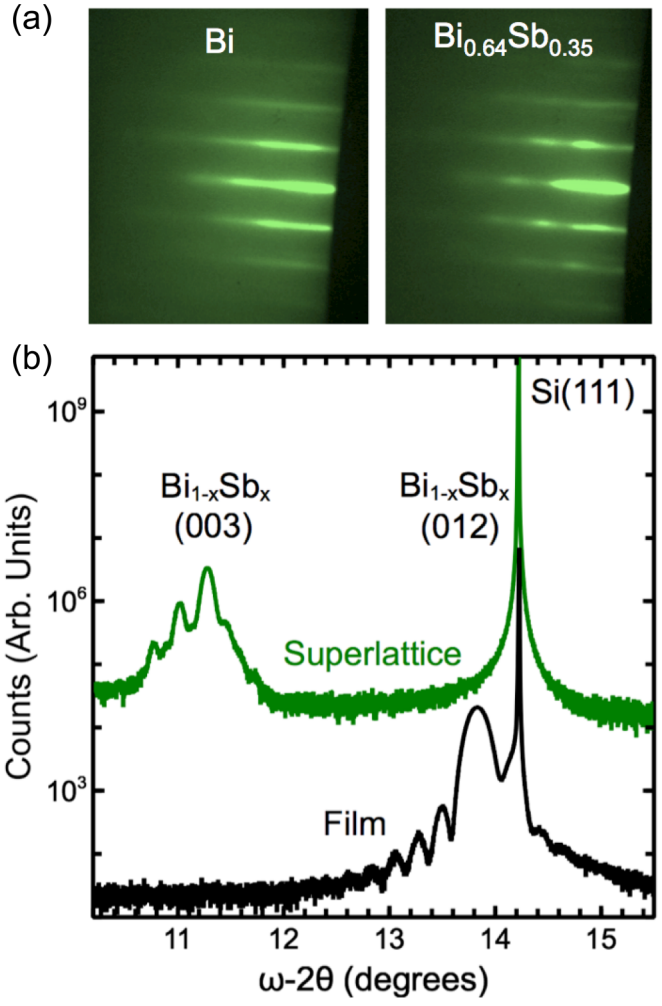

FIG. 4. (a) RHEED measurements of $Bi/Bi_{0.64}Sb_{0.36}$ superlattice indicating 1×1 reconstruction in both Bi and $Bi_{0.64}Sb_{0.36}$ layers. (b) XRD measurements of $Bi/Bi_{0.64}Sb_{0.36}$ superlattice and $Bi_{0.64}Sb_{0.36}$ film indicating (001) orientation maintained in superlattice.

during *ex situ* measurement; however, the oxide/film ratio in XPS measurements is quite similar, and no oxide peaks are present in wide-angle XRD. As the conductivity and surface roughness of both orientations are comparable, significant hopping transport also appears unlikely. Another possibility is that a larger band gap in the $Bi_{1-x}Sb_x(012)$ films opened by Sb alloying results in domination of the quantum confined bulk states even in thinner films. However, the consistency of the temperature dependence between 9 and 28% Sb, the latter of which is outside the bulk semiconducting regime, makes this unlikely. *In situ* ARPES or magnetotransport measurements of $Bi_{1-x}Sb_x(012)$ could help to clarify the origin of this behavior. Regardless, the absence of the characteristic metallic surface-state conductivity in $Bi_{1-x}Sb_x(012)$ indicates that the orientation transition may restrict transport measurements of TI surface states in $Bi_{1-x}Sb_x(001)/Si(111)$.

As illustrated in Fig. 4, growth of the $Bi_{1-x}Sb_x$ film on a Bi buffer layer or in a $Bi/Bi_{1-x}Sb_x$ superlattice is a potential solution for measuring $Bi_{1-x}Sb_x(001)$ within the TI regime on Si(111). RHEED measurements comparing Bi and $Bi_{0.64}Sb_{0.36}$ layers of a five-layer $Bi/Bi_{0.64}Sb_{0.36}$ superlattice in Fig. 4(a) demonstrate that the underlying Bi buffer layer can assist in maintaining a 1×1 reconstruction in the $Bi_{0.64}Sb_{0.36}$ layers. Each layer of the measured superlattice is 10 nm. XRD measurements of the $Bi/Bi_{0.64}Sb_{0.36}$ superlattice and a reference 20-nm $Bi_{0.64}Sb_{0.36}$ film in Fig. 4(b) indicate that, while the $Bi_{0.64}Sb_{0.36}/Si(111)$ film is (012) oriented, the $Bi/Bi_{0.64}Sb_{0.36}$ superlattice maintains a (001) orientation. The distinct superlattice peaks surrounding the main (003) peak suggest that the integrity of the layers is maintained, without significant interdiffusion. This result explains the measurement of $Bi_{1-x}Sb_x$ in the TI regime by Benia *et al.*; as the $Bi_{1-x}Sb_x$ films are grown on a 30-nm Bi buffer layer on Si(111), the (001) orientation is maintained [15]. While this approach is promising for ARPES measurements, isolating the $Bi_{1-x}Sb_x$ transport from the Bi buffer layer is likely to remain challenging.

Finally, focusing on $Bi_{1-x}Sb_x$ films thinner than 4 nm, in which the A17 structure is expected in Bi, we find in Fig. 5 that alloying with Sb improves the continuity and quality of nanoscale $Bi_{1-x}Sb_x(012)$ films. The A17 Bi(012) phase forms even-monolayer, small-area islands, which coalesce and form a continuous film immediately before the allotropic transition to A7 Bi(001) [27–30,50]. From the high-resolution AFM measurements shown in Fig. 5(a), we find that alloying with 26% Sb decreased the island area in the 3-ML film, resulting in a higher density of smaller islands. Similar to the effect of lowering the substrate temperature [27], the close-packed nature of the $Bi_{0.74}Sb_{0.26}(012)$ islands facilitates earlier coalescence, lowering the surface roughness by almost half compared to Bi(012) by 4 nm of growth. As demonstrated in Fig. 5(b), the conductivity of the $Bi_{0.74}Sb_{0.26}$ films, which is normalized to the 50-nm value in order to exclude the dependence of the conductivity on the composition-dependent band structure, does not degrade with decreasing film thickness, in contrast to the behavior of Bi. The conductivity of $Bi_{0.74}Sb_{0.26}$ films as thin as 4 nm is able to be measured successfully, while Bi films sharply increase in resistance below the critical thickness. This result indicates that Sb alloying improves the continuity of ultrathin $Bi_{1-x}Sb_x(012)$ on Si(111) compared to pure Bi. If the A17 allotrope is indeed stable in nanoscale $Bi_{1-x}Sb_x$ on Si(111), as is suggested by the similarity of the early growth process to pure Bi, the (012) orientation of ultrathin films, and the weak adhesion of $Bi_{1-x}Sb_x(001)$ to the substrate, Sb alloying could be a promising approach toward compositional tuning of high-quality puckered-layer A17 Bi.

III. CONCLUSION

In conclusion, we demonstrate that epitaxial $Bi_{1-x}Sb_x$ on Si(111) undergoes an orientation change at concentrations above 8–9% Sb, due to suppression of the A17 Bi(012) to A7 Bi(001) allotropic transition. The transition to $Bi_{1-x}Sb_x(012)$ overlaps with the TI composition regime in bulk crystals (7–22% Sb), and is found to reduce the characteristic temperature-dependent conductivity of the surface states in thin films. Growth on a Bi(001) buffer layer may be a suitable method for maintaining the (001) orientation within the TI composition regime. We further demonstrate that Sb alloying results in earlier coalescence of the 2D $Bi_{1-x}Sb_x(012)$ islands,

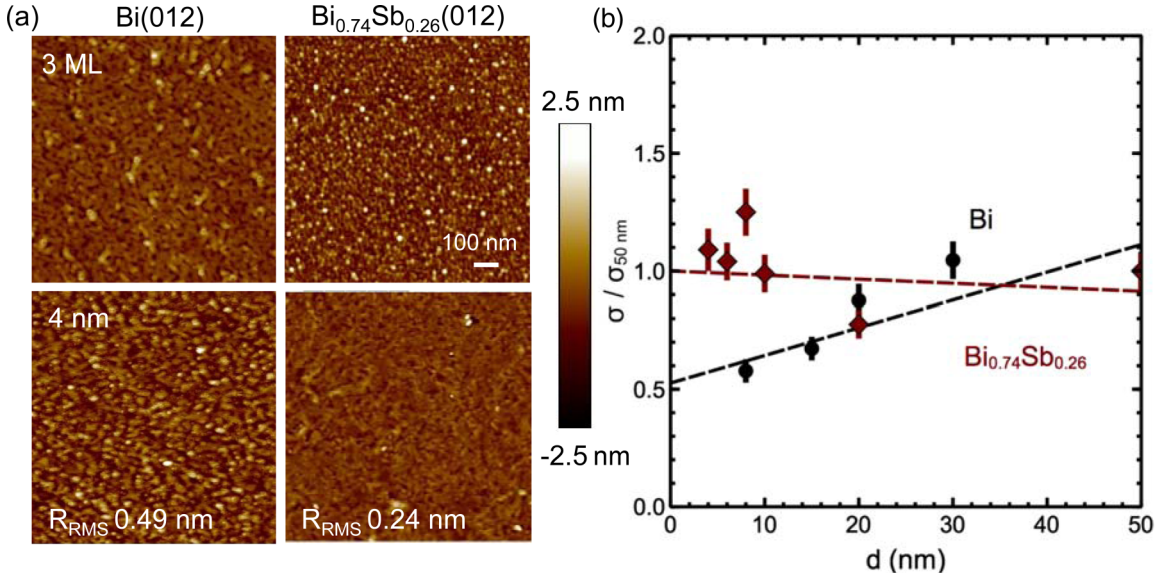

FIG. 5. (a) AFM measurements of 3-ML and 4-nm Bi(012) and $Bi_{0.74}Sb_{0.26}$(012) showing higher density islands and lower surface roughness in $Bi_{0.74}Sb_{0.26}$(012). (b) Conductivity measurements of Bi and $Bi_{0.74}Sb_{0.26}$ normalized to the conductivity at 50 nm.

facilitating electrical measurements of ultrathin films and providing a promising route toward investigating the unique electronic properties of puckered-layer $Bi_{1-x}Sb_x$(012).

ACKNOWLEDGMENTS

This work was primarily supported by both the Texas Instruments Semiconductor Research Corporation Graduate Fellowship Program and the National Science Foundation through the Center for Dynamics and Control of Materials, an NSF MRSEC under Cooperative Agreement No. DMR-1720595. The authors would like to acknowledge Dr. H. Celio from the Texas Materials Institute at the University of Texas at Austin for assistance with x-ray photoelectron spectroscopy, and Prof. D. Milliron and C. Staller from the Department of Chemical Engineering at the University of Texas at Austin for assistance with electrical measurements.

[1] B. Lenoir, M. Cassart, J.-P. Michenaud, H. Scherrer, and S. Scherrer, Transport properties of Bi-rich Bi-Sb alloys, J. Phys. Chem. Solids **57**, 89 (1996).

[2] D. Hsieh, D. Qian, L. Wray, Y. Xia, Y. S. Hor, R. J. Cava, and M. Z. Hasan, A topological Dirac insulator in a quantum spin Hall phase, Nature (London) **452**, 970 (2008).

[3] H.-J. Zhang, C.-X. Liu, X.-L. Qi, X. Dai, Z. Fang, and S.-C. Zhang, Topological insulators in Bi_2Se_3, Bi_2Te_3 and Sb_2Te_3 with a single Dirac cone on the surface, Nat. Phys. **5**, 438 (2009).

[4] X. Liu, D. J. Smith, J. Fan, Y.-H. Zhang, H. Cao, Y. P. Chen, J. Leiner, B. J. Kirby, M. Dobrowolska, and J. K. Furdyna, Structural properties of Bi_2Te_3 and Bi_2Se_3 topological insulators grown by molecular beam epitaxy on GaAs(001) substrates, Appl. Phys. Lett. **99**, 171903 (2011).

[5] Y. S. Kim, M. Brahlek, N. Bansal, E. Edrey, G. A. Kapilevich, K. Iida, M. Tanimura, Y. Horibe, S.-W. Cheong, and S. Oh, Thickness-dependent bulk properties and weak antilocalization effect in topological insulator Bi_2Se_3, Phys. Rev. B **84**, 073109 (2011).

[6] N. Bansal, Y. S. Kim, M. Brahlek, E. Edrey, and S. Oh, Thickness-Independent Transport Channels in Topological Insulator Bi_2Te_3 Thin Films, Phys. Rev. Lett. **109**, 116804 (2012).

[7] A. Roy, S. Guchhait, S. Sonde, R. Dey, T. Pramanik, A. Rai, H. C. P. Movva, L. Colombo, and S. K. Banerjee, Two-dimensional weak anti-localization in Bi_2Te_3 thin film grown on Si(111)-(7×7) surface by molecular beam epitaxy, Appl. Phys. Lett. **102**, 163118 (2013).

[8] C. Klein, M. Vyshnepolsky, A. Kompch, F. Klasing, A. Hanisch-Blicharski, M. Winterer, and M. Horn-von Hoegen, Strain state, film and surface morphology of epitaxial topological insulator Bi_2Se_3 films on Si(111), Thin Solid Films **564**, 241 (2014).

[9] T. P. Ginley and S. Law, Growth of Bi_2Se_3 topological insulator films using a selenium cracker source, J. Vac. Sci. Technol. B **34**, 02L105 (2016).

[10] T. Trivedi, A. Roy, H. C. P. Movva, E. S. Walker, S. R. Bank, D. P. Neikirk, and S. K. Banerjee, Versatile large-area custom-feature van der Waals epitaxy of topological insulators, ACS Nano **11**, 7457 (2017).

[11] J. C. Y. Teo, L. Fu, and C. L. Kane, Surface states and topological invariants in three-dimensional topological insulators: Application to $Bi_{1-x}Sb_x$, Phys. Rev. B **78**, 045426 (2008).

[12] A. A. Taskin and Y. Ando, Quantum oscillations in a topological insulator $Bi_{1-x}Sb_x$, Phys. Rev. B **80**, 085303 (2009).

[13] H.-J. Zhang, C.-X. Liu, X.-L. Qi, X.-Y. Deng, X. Dai, S.-C. Zhang, and Z. Fang, Electronic structures and surface states

of the topological insulator $Bi_{1-x}Sb_x$, Phys. Rev. B **80**, 085307 (2009).

[14] F. Nakamura, Y. Kousa, A. A. Taskin, Y. Takeichi, A. Nishide, A. Kakizaki, M. D'Angelo, P. Lefevre, F. Bertran, A. Taleb-Ibrahimi *et al.*, Topological transition in $Bi_{1-x}Sb_x$ studied as a function of Sb doping, Phys. Rev. B **84**, 235308 (2011).

[15] H. M. Benia, C. Strasser, K. Kern, and C. R. Ast, Surface band structure of $Bi_{1-x}Sb_x(111)$, Phys. Rev. B **91**, 161406(R) (2015).

[16] Y. Ueda, N. H. D. Khang, K. Yao, and P. N. Hai, Epitaxial growth and characterization of $Bi_{1-x}Sb_x$ spin Hall thin films on GaAs(111)A substrates, Appl. Phys. Lett. **110**, 062401 (2017).

[17] N. H. D. Khang, Y. Ueda, and P. N. Hai, A conductive topological insulator with colossal spin Hall effect for ultra-low power spin-orbit-torque switching, Nat. Mater. **17**, 808 (2018).

[18] D. Shin, Y. Lee, M. Sasaki, Y. H. Jeong, F. Weickert, J. B. Betts, H.-J. Kim, K.-S. Kim, and J. Kim, Violation of Ohm's law in a Weyl metal, Nat. Mater. **16**, 1096 (2017).

[19] Y.-H. Su, W. Shi, C. Felser, and Y. Sun, Topological Weyl semimetals in $Bi_{1-x}Sb_x$ alloys, Phys. Rev. B **97**, 155431 (2018).

[20] T. Hirahara, K. Miyamoto, I. Matsuda, T. Kadono, A. Kimura, T. Nagao, G. Bihlmayer, E. Chulkov, S. Qiao, K. Shimada *et al.*, Direct observation of spin splitting in bismuth surface states, Phys. Rev. B **76**, 153305 (2007).

[21] N. Marcano, S. Sangiao, C. Magén, L. Morellón, M. R. Ibarra, M. Plaza, L. Pérez, and J. M. De Teresa, Role of the surface states in the magnetotransport properties of ultrathin bismuth films, Phys. Rev. B **82**, 125326 (2010).

[22] M. Aitani, T. Hirahara, S. Ichinokura, M. Hanaduka, D. Shin, and S. Hasegawa, *In situ* Magnetotransport Measurements in Ultrathin Bi Films: Evidence for Surface-Bulk Coherent Transport, Phys. Rev. Lett. **113**, 206802 (2014).

[23] M. Y. Tang and M. S. Dresselhaus, A band structure phase diagram calculation of 2D BiSb films, MRS Proc. **886**, 0886-F04-05 (2005).

[24] T. Hirahara, Y. Sakamoto, Y. Saisyu, H. Miyazaki, S. Kimura, T. Okuda, I. Matsuda, S. Murakami, and S. Hasegawa, Topological metal at the surface of an ultrathin $Bi_{1-x}Sb_x$ alloy film, Phys. Rev. B **81**, 165422 (2010).

[25] M. Kammler and M. Horn-von Hoegen, Low energy electron diffraction of epitaxial growth of bismuth on Si(111), Surf. Sci. **576**, 56 (2005).

[26] C. G. Tan, P. Zhou, J. G. Lin, and L. Z. Sun, Prediction of two-dimensional BiSb with puckered structure, Phys. Status Solidi RRL **11**, 1700051 (2017).

[27] T. Nagao, J. Sadowski, M. Saito, S. Yaginuma, Y. Fujikawa, T. Kogure, T. Ohno, Y. Hasegawa, S. Hasegawa, and T. Sakurai, Nanofilm Allotrope and Phase Transformation of Ultrathin Bi Film on Si(111)-7×7, Phys. Rev. Lett. **93**, 105501 (2004).

[28] T. Nagao, S. Yaginuma, M. Saito, T. Kogure, J. T. Sadowski, T. Ohno, S. Hasegawa, and T. Sakurai, Strong lateral growth and crystallization via two-dimensional allotropic transformation of semi-metal Bi film, Surf. Sci. **590**, 247 (2005).

[29] S. Yaginuma, T. Nagao, J. T. Sadowski, M. Saito, K. Nagaoka, Y. Fujikawa, T. Sakurai, and T. Nakayama, Origin of flat morphology and high crystallinity of ultrathin bismuth films, Surf. Sci. **601**, 3593 (2007).

[30] J. T. Sadowski, T. Nagao, S. Yaginuma, Y. Fujikawa, and T. Sakurai, Stability of the quasicubic phase in the initial stage of the growth of bismuth films on Si(111)-7×7, J. Appl. Phys. **99**, 014904 (2006).

[31] S. Yaginuma, K. Nagaoka, T. Nagao, G. Bihlmayer, Y. M. Koroteev, E. V. Chulkov, and T. Nakayama, Electronic structure of ultrathin bismuth films with A7 and black-phosphorus-like structures, J. Phys. Soc. Jpn. **77**, 014701 (2008).

[32] E. Aktürk, O. Ü. Aktürk, and S. Ciraci, Single and bilayer bismuthene: Stability at high temperature and mechanical and electronic properties, Phys. Rev. B **94**, 014115 (2016).

[33] J. T. Sun, H. Huang, S. L. Wong, H. J. Gao, Y. P. Feng, and A. T. S. Wee, Energy-Gap Opening in a Bi(110) Nanoribbon Induced by Edge Reconstruction, Phys. Rev. Lett. **109**, 246804 (2012).

[34] S. Xiao, D. Wei, and X. Jin, Bi(111) Thin Film with Insulating Interior But Metallic Surfaces, Phys. Rev. Lett. **109**, 166805 (2012).

[35] E. S. Walker, S. R. Na, D. Jung, S. D. March, J.-S. Kim, T. Trivedi, W. Li, L. Tao, M. L. Lee, K. M. Liechti *et al.*, Large-area dry transfer of single-crystalline epitaxial bismuth thin films, Nano Lett. **16**, 6931 (2016).

[36] E. Tournié and K. H. Ploog, Virtual-surfactant epitaxy of strained $InAs/Al_{0.48}In_{0.52}As$ quantum wells, Appl. Phys. Lett. **62**, 858 (1993).

[37] E. Tournié, N. Grandjean, A. Trampert, J. Massies, and K. H. Ploog, Surfactant-mediated molecular-beam epitaxy of III-V strained-layer heterostructures, J. Cryst. Growth **150**, 460 (1995).

[38] J. A. van Hulst, H. M. Jaeger, and S. Radelaar, Epitaxial growth of bismuth films and bismuth-antimony heterostructures, Phys. Rev. B **52**, 5953 (1995).

[39] See Supplemental Material at http://link.aps.org/supplemental/10.1103/PhysRevMaterials.3.064201 for information regarding $Bi_{1-x}Sb_x$ composition calibration, surface droplet formation in pure Bi, and extended materials characterization.

[40] M. Fortin-Deschenes, O. Waller, T. O. Mentes, A. Locatelli, S. Mukherjee, F. Genuzio, P. L. Levesque, A. Hebert, R. Martel, and O. Moutanabbir, Synthesis of antimonene on germanium, Nano Lett. **17**, 4970 (2017).

[41] S. Cho, A. Divenere, G. K. Wong, J. B. Ketterson, and J. R. Meyer, Molecular beam epitaxial growth and structural properties of $Bi_{1-x}Sb_x$ alloy thin films on CdTe(111) substrates, J. Vac. Sci. Technol. A **17**, 9 (1999).

[42] J. D. Caldwell, T. J. Anderson, J. C. Culbertson, G. G. Jernigan, K. D. Hobart, F. J. Kub, M. J. Tadjer, J. L. Tedesco, J. K. Hite, M. A. Mastro *et al.*, Technique for the dry transfer of epitaxial graphene onto arbitrary substrates, ACS Nano **4**, 1108 (2010).

[43] T. Nagao, T. Doi, T. Sekiguchi, and S. Hasegawa, Epitaxial growth of single-crystal ultrathin films of bismuth on Si(111), Jpn. J. Appl. Phys. **39**, 4567 (2000).

[44] V. B. Sandomirskii, Quantum size effect in a semimetal film, Sov. Phys. JETP **25**, 101 (1967).

[45] G. E. Smith, G. A. Baraff, and J. M. Rowell, Effective g factor of electrons and holes in bismuth, Phys. Rev. **135**, A1118 (1964).

[46] Y. M. Koroteev, G. Bihlmayer, J. E. Gayone, E. V. Chulkov, S. Blügel, P. M. Echenique, and Ph. Hofmann, Strong Spin-Orbit Splitting on Bi Surfaces, Phys. Rev. Lett. **93**, 046403 (2004).

[47] Y. Koroteev, G. Bihlmayer, E. Chulkov, and S. Blügel, First-principles investigation of structural and electronic properties of ultrathin Bi films, Phys. Rev. B **77**, 045428 (2008).

[48] J. I. Pascual, G. Bihlmayer, Y. Koroteev, H.-P. Rust, G. Ceballos, M. Hansmann, K. Horn, E. Chulkov, S. Blügel, P. Echenique, and P. Hofmann, Role of Spin in Quasiparticle Interference, Phys. Rev. Lett. **93**, 196802 (2004).

[49] S. Agergaard, C. Sondergaard, H. Li, M. B. Nielsen, S. V Hoffmann, Z. Li, P. Hofmann, and S. S Agergaard, The effect of reduced dimensionality on a semimetal: the electronic structure of the Bi(110) surface, New J. Phys. **3**, 15 (2001).

[50] M. Saito, T. Ohno, and T. Miyazaki, Magic layer thickness in Bi ultrathin films on Si(111) surface, Appl. Surf. Sci. **237**, 80 (2004).